remote sensing

MDPI

Article

Impervious Surface Area Changes and Urban Expansion in China's Three Major Urban Agglomerations over the Past 40 Years

Fei Wang [1,*], Yumeng Yang [2], Lei Yu [1], Fengyun Sang [1], Yaning Chen [3] and Siquan Yang [4]

[1] Information Institute of the Ministry of Emergency Management of the PRC, Beijing 100029, China; yulei@iiem.ac.cn (L.Y.); sangfy@iiem.ac.cn (F.S.)
[2] Department of Big Data Development, State Information Center, Beijing 100045, China; yangyumeng@sic.gov.cn
[3] Xinjiang Institute of Ecology and Geography, Chinese Academy of Sciences, Urumqi 830011, China; chenyn@ms.xjb.ac.cn
[4] National Institute of Natural Hazards, Ministry of Emergency Management of China, Beijing 100085, China; siquanyang@ninhm.ac.cn
* Correspondence: wangfei@iiem.ac.cn

Highlights

What are the main findings?

- Between 1985 and 2024, the impervious surface area of China's three major urban agglomerations expanded from 22,544.10 km^2 to 69,348.59 km^2. Despite this substantial growth, both the expansion rate and intensity have exhibited a distinct decelerating trend. This shift signifies a fundamental transition in the development paradigm, moving away from rapid urbanization driven by incremental expansion and toward an adjacency-dominated, infill-oriented expansion.
- LCI-based analysis of urban expansion across five megacities reveals that adjacency expansion type has become the predominant form of growth, exceeding 50% in most cities. This signifies a clear shift toward infill and contiguous development anchored to the peripheries of existing built-up areas.

What are the implications of the main findings?

- The main findings reveal the refined evolutionary trajectories of impervious surface area in China's three major urban agglomerations spanning 1985–2024.
- The main findings also offer informative insights that can be used to guide regionally differentiated urban planning policies, urban resilience construction, and sustainable land management strategies.

Abstract

Analyzing the impervious surface area (ISA) of China's three major urban agglomerations and expansion pattern of representative cities is of great significance for formulating context-specific urban planning policies and enhancing the resilience of urban development. This research employs impervious surface expansion indicators to reveal the spatiotemporal dynamics of impervious surface area, and further applies the location centrality index (LCI) to investigate the expansion structures and patterns of five megacities. The results indicate that the ISA of China's three major urban agglomerations expanded from 22,544.10 km^2 to 69,348.59 km^2 from 1985 to 2024; both the expansion rate and intensity have exhibited a distinct decelerating trend. However, significant regional variation exists in the peak expansion phases: the Guangdong–Hong Kong–Macao Greater Bay Area Urban Agglomeration (GBA) peaked during the Initial Exploratory Phase (1985–1995), whereas the Yangtze

Check for updates

Academic Editor: Tania Stathaki

Received: 30 April 2026
Revised: 26 June 2026
Accepted: 1 July 2026
Published: 6 July 2026

Copyright: © 2026 by the authors. Licensee MDPI, Basel, Switzerland. This article is an open access article distributed under the terms and conditions of the Creative Commons Attribution (CC BY) license.

River Delta Urban Agglomeration (YRD) and Beijing–Tianjin–Hebei Urban Agglomeration (BTH) reached their peaks during the High-speed Development Phase (2005–2015). At the urban scale, LCI-based analysis of urban expansion across five megacities reveals that adjacency expansion type has become the predominant form of growth, exceeding 50% in most cities. These findings enhance our understanding of evolutionary trajectories of ISA within urban agglomerations and the expansion patterns of five megacities, providing a scientific basis for sustainable urban planning and urban resilience.

Keywords: impervious surface area; spatiotemporal variations; expansion pattern; urban agglomerations

1. Introduction

Since the initiation of its reform and opening-up policy in 1978, China has undergone an urbanization process unprecedented in world history in both scale and pace [1]. The urbanization rate surged from 17.9% in 1978 to 67% in 2024 [2,3], with the urban population exceeding 940 million [3,4]. In 2017, the Chinese government explicitly proposed an urbanization strategy that positions urban agglomerations as the principal form [5]. In August 2025, the *Guiding Opinions on Promoting High-Quality Urban Development* was issued and outlined the development of clustered and networked modern urban agglomerations and metropolitan areas [6]. It emphasized supporting the BTH, YRD, and GBA in building world-class urban agglomerations. These three major urban agglomerations, occupying approximately 5% of the nation's land area [7–9], accommodate about 30% of the population [9,10] and contribute about 44% of the GDP [10,11], making them a core engine of China's economic development [12]. However, despite sharing the same national strategic direction, they are likely to exhibit significantly different patterns and morphologies of spatial variations due to varying natural geographical conditions, economic development stages, and regional governance models [13,14]. Thus, a comparative analysis of the spatiotemporal variations in major urban agglomerations is critical for understanding their developmental dynamics and formulating differentiated urbanization strategies.

Impervious surface area changes and urban expansion constitute a focal research domain in urban geography. Research on impervious surface area changes has primarily focused on spatiotemporal variations, driving mechanisms, and land use impacts of impervious surface expansion. In terms of spatiotemporal variations, impervious surfaces, as the most intuitive physical representation of land cover in urban areas, have been widely used as effective indicators for assessing the development level and quality of urban agglomerations [15–18]. Numerous studies have revealed the expansion rates and spatial patterns of impervious surfaces at different scales based on time-series remote sensing images. At the urban agglomeration scale, Zhang et al. [19] developed a novel method using semi-supervised SVM and seasonal time-series indices, revealing that impervious surfaces in the Wuhan urban agglomeration increased by 20.10% annually from 2000 to 2016. And Zhang et al. [20] proposed an integrated "clustering + accessibility" framework to identify urban agglomeration ranges, which effectively captured the dynamic spatial evolution of the Central Yunnan Urban Agglomeration from 2014 to 2022. From an urban perspective, Xu et al. [21] analyzed the changes in impervious surface density in Guangzhou from 1987 to 2019 using an inverse S-shaped urban impervious surface density function, finding that the urban spatial structure transitioned from monocentric to polycentric. Man et al. [22] demonstrated that the spatial patterns of impervious surfaces in Xiamen exhibit fractal and multifractal characteristics, with increasing fractal dimensions from 1994 to 2015 indicating growing complexity and clustering,

while multifractal analysis reveals persistent spatial heterogeneity. Zhang et al. [23] examined impervious surface data for the Yellow River Basin from 1986 to 2020, showing that the ISA increased from 2513.71 km^2 to 18,287.36 km^2, with the expansion rate accelerating in stages and varying between core urban areas and rural areas. Regarding the driving mechanisms, scholars generally agree that impervious surface area changes are influenced by both natural and socio-economic factors [24]. Natural factors include topography [25], climate [26], hydrological conditions [27], and surface environmental characteristics [28,29]. Socio-economic factors are regarded as the primary driving forces, encompassing economic growth, population increase [30], transportation infrastructure development [31], and policy guidance [32]. A study by Zou et al. [33] on the Pearl River Delta urban agglomeration demonstrated that the Geographically and Temporally Weighted Regression model reveals significant spatial heterogeneity in natural constraints such as elevation and river network density, while socio-economic drivers such as road area and foreign direct investment serve as core catalysts for impervious surface expansion. More importantly, policy factors fundamentally determine the direction and intensity of impervious surface area changes, and numerous studies have confirmed that the phased advancement of regional policies plays a key regulatory role in impervious surface growth [34–38]. On the land use impacts of impervious surface expansion, Li et al. [39] examined the relationship between impervious surface and flood risk across urban agglomerations in the Yangtze River Basin, identifying how topographical and infrastructural conditions moderate land use impacts, revealing that the Chengdu–Chongqing agglomeration showed a negative correlation, while a weak positive correlation was observed for the urban agglomeration in the middle reaches of the Yangtze River.

Research on urban expansion both domestically and internationally is the basis for the selection of indices and models, and urban expansion patterns. For the indices and models, researchers have developed various methods for quantitatively characterizing urban expansion features, such as the urban expansion efficiency indicators [40], urban growth metrics [41], landscape indices [42], and expansion identification models based on nighttime light data or population density grids [43,44]. Particularly in the YRD, a Comprehensive Nighttime Light Index was constructed to systematically analyze the spatiotemporal dynamics of urban expansion; Shao et al. [45] found that the regional spatial structure progressively transitioned from an early "pole-core-belt" pattern to a polycentric urban agglomeration system. Concerning urban expansion, an analysis of global major urban expansion by Xia et al. [46] indicated that urban expansion in high-income countries was predominantly infill expansion. Li et al. [47] analyzed five major urban agglomerations in China and found that the Pearl River Delta and Yangtze River Delta had higher degrees of urbanization than the Beijing–Tianjin–Hebei, Chengdu–Chongqing, and Middle Reaches of the Yangtze River urban agglomerations, with polycentric regions demonstrating a significant siphoning effect. Furthermore, recent studies on major urban agglomerations in China showed that urban expansion exhibited typical characteristics such as staged development, polycentric and networked patterns, and transportation orientation [48,49].

Despite significant advances in the study of impervious surface and urban expansion across major urban agglomerations in China, critical scientific bottlenecks remain to be urgently addressed. First, most studies focus on a single urban agglomeration or short time series analyses, lacking long-term, comparative research across multiple agglomerations, thus failing to capture the commonalities and specificities inherent in the development patterns of different urban agglomerations. Second, traditional approaches to analyzing urban expansion, which often utilize the landscape expansion index (LEI) and its derivative index [50–52], depend on localized neighborhood pixels. Consequently, these indices primarily reflect the expansion of new patches relative to the nearest old patches, lacking a comprehensive analysis of the overall expansion structure [53,54]. To address

this limitation, this study conducts a comparative analysis of long time series impervious surface areas dynamics across China's three major urban agglomerations, while simultaneously employing the LCI to further investigate the urban expansion characteristics of five megacities [55]. This research makes two primary contributions. First, through a 40-year comparative analysis of impervious surface area changes, it reveals the phased differences and convergence characteristics of the expansion processes across different urban agglomerations, thereby overcoming the limitations of previous studies that lacked long-time series and multi-urban agglomeration comparisons. Second, we apply the LCI to a comparative study of five megacities, compensating for the shortcomings of traditional methods. By employing the "area-inverse distance" weighting algorithm, the LCI comprehensively identifies the centrality of the new patches when compared with the locations of main centers, subcenters, or potential centers [55].

The main purpose of this research was to characterize the spatiotemporal variations of ISA and urban expansion within three major urban agglomerations in China, with a particular focus on their five core megacities. To this end, long time series remote sensing data from 1985 to 2024 were used. The research framework of this study is illustrated in Figure 1. This research included: (1) a multi-scale spatiotemporal analysis of ISA across the three urban agglomerations using the impervious surface expansion indicators; (2) the application of LCI to quantitatively characterize the structural patterns of urban expansion specifically within the five aforementioned megacities; and (3) an analysis of development pathways across different stages of urbanization, integrating macro-level urban agglomeration trends with micro-level of representative megacities. Through the use of these methods, this research seeks to clarify the evolutionary characteristics of China's three major urban agglomerations and the urban expansion of five megacities, providing a scientific basis for sustainable urban planning and urban resilience.

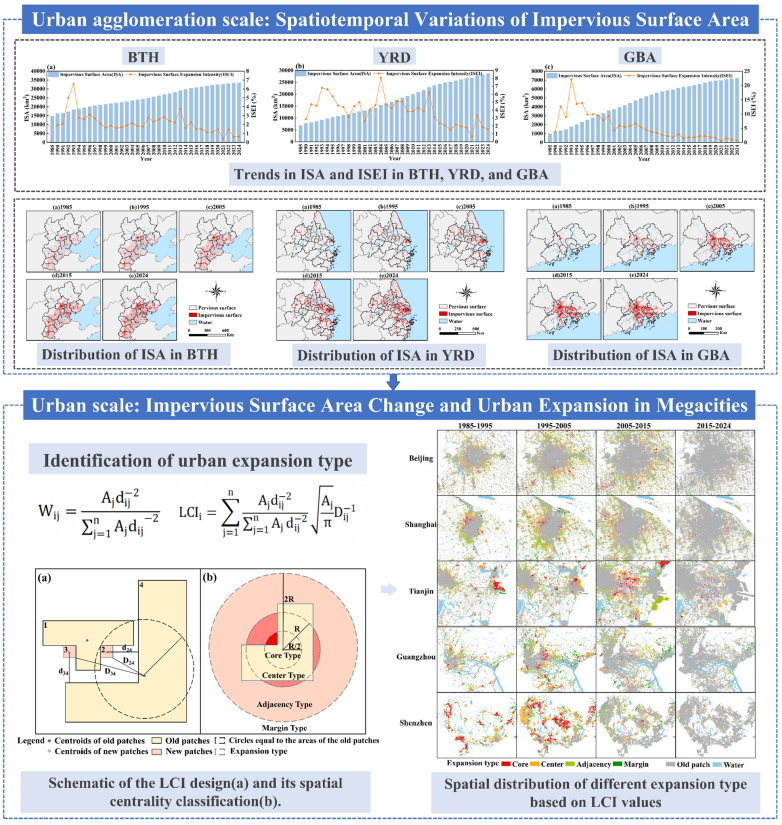


Figure 1. Research framework flowchart.

2. Materials and Methods

2.1. Study Area Overview

This study selects the BTH, YRD, and GBA as its research subjects, as shown in Figure 2. These three urban agglomerations serve as highly representative cases, as they are the earliest developed, largest, and most rapidly and extensively urbanized regions in China. Accounting for over 40% of the national economic output, they have established themselves as world-class urban agglomerations with robust global competitiveness.

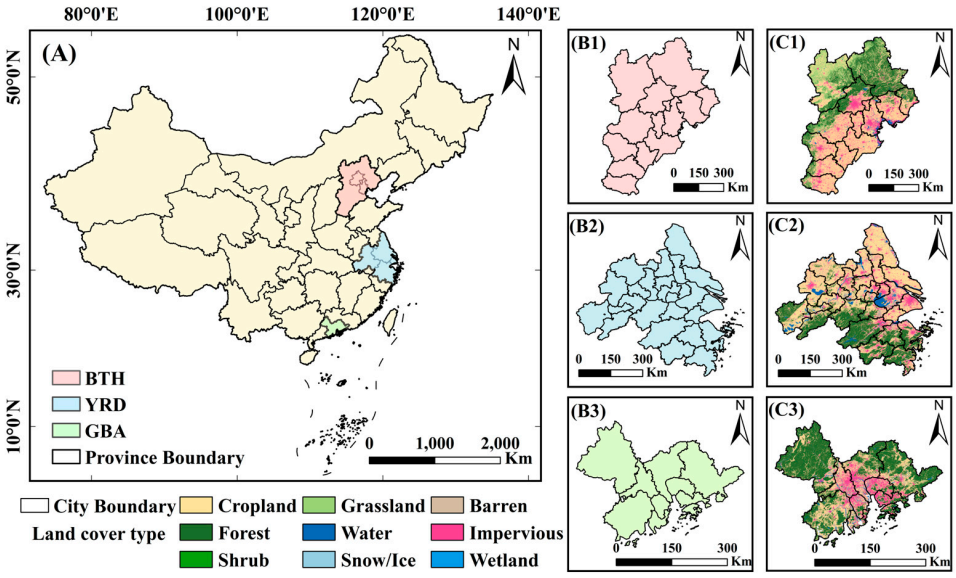


Figure 2. Study area: (**A**) the locations of the three major urban agglomerations in China; (**B1**–**B3**) administrative division maps of the BTH, YRD, and GBA regions; (**C1**–**C3**) land cover type maps of BTH, YRD, and GBA in 2024.

2.1.1. Beijing–Tianjin–Hebei Urban Agglomeration (13 Cities)

The BTH is located between 36°05′N to 42°40′N and 113°27′E to 119°50′E, encompassing Beijing, Tianjin, and 11 prefecture-level cities in Hebei Province, including Shijiazhuang, Tangshan, and Baoding. Covering a total area of 216,000 square kilometers [7], the region has a permanent population of approximately 109 million [10]. In 2024, its regional GDP reached 11.5 trillion yuan [10]. The spatial evolution of the BTH is characterized by a transition from a monocentric structure dominated by Beijing to a polycentric, networked pattern. Strategically, this development focuses on establishing the Xiong'an New Area and the Beijing Municipal Administrative Center as its "two wings". The former serves as the primary destination for the relocation of Beijing's non-capital functions, while the latter aims to optimize the spatial layout within the municipality.

2.1.2. Yangtze River Delta Urban Agglomeration (26 Cities)

The YRD is located between 29°20′N to 32°34′N and 115°46′E to 123°25′E. Its designated region comprises 26 cities, including Shanghai, Nanjing, Wuxi, Suzhou, Hangzhou, Ningbo, Hefei et al. The total area of the YRD is 211,700 square kilometers [8]. In 2024, its permanent resident population reached 238 million [10], and its regional GDP amounted to 33.17 trillion yuan [10]. The spatial structure of the YRD is characterized by a polycentric and networked pattern rather than a monocentric one. Spearheaded by Shanghai and bolstered by other major cities with GDPs exceeding one trillion yuan, such as Nanjing, Hangzhou, Suzhou, and Hefei, the region demonstrates a high degree of interdependence among its municipalities.

2.1.3. Guangdong–Hong Kong–Macao Greater Bay Area Urban Agglomeration (11 Cities)

The GBA is situated between 21°48′N to 23°34′N and 112°03′E to 114°30′E. It encompasses nine cities in Guangdong Province—including Guangzhou, Shenzhen, Zhuhai, Foshan, among others—as well as the Hong Kong and Macao Special Administrative Regions, covering a total area of approximately 56,000 square kilometers [9]. In 2024, the population of the GBA exceeded 87 million [9], and its regional GDP reached 14.79 trillion yuan [11]. As a primary landfall zone for typhoons in the northwestern Pacific, the region is frequently affected by typhoon-induced storm surges and associated hazards. The spatial layout of the GBA emphasizes synergistic development among major growth poles, such as Hong Kong-Shenzhen, Guangzhou-Foshan, and Macao-Zhuhai, supported by development corridors that radiate influence throughout the region.

2.2. Data Sources

The data source for this study is the Landsat-derived annual China Land Cover Dataset (CLCD), derived from Landsat images via the Google Earth Engine (GEE) platform (https://doi.org/10.5281/zenodo.15853565, accessed on 13 August 2025). The CLCD dataset was constructed by combining stable samples extracted from China's land use/cover datasets (CLUDs) and visually interpreted samples from satellite time-series data Using 335,709 Landsat images on GEE, a set of spectral, phenological and topographical metrics was calculated via pixel-wise temporal composites. Several temporal metrics were then constructed and fed into the Random Forest classifier to obtain classification results. A spatial–temporal post-processing method incorporating spatial–temporal filtering, and logical reasoning was proposed to further improve the spatial–temporal consistency of CLCD. Based on 5463 visually interpreted samples, the overall accuracy of CLCD reached 79.31%. The CLCD dataset provides annual LULC classification products at a 30 m spatial resolution spanning the period from 1985 to 2024 [56,57], encompassing nine distinct types: Cropland, Forest, Shrub, Grassland, Water, Snow/Ice, Barren, Impervious, and wetland. In addition, the impervious surface area derived from CLCD (CLCD-ISA) was intercompared with the existing well-known 30 m annual ISA products (i.e., GISA, GAUD, GAIA). Given that all these products are derived from remote sensing data, this comparison serves as a cross-dataset consistency assessment. The CLCD-ISA exhibited good consistency with the existing ISA products ($0.51 < R^2 < 0.83$), which indicates the relative reliability of CLCD products. And the CLCD-ISA data encompass rural areas [56]. Based on this dataset, this study extracted annual CLCD-ISA data for the three major urban agglomerations (the BTH, YRD, and GBA) from 1985 to 2024, with a particular focus on characterizing the spatiotemporal evolution of ISA in five megacities.

2.3. Methods

2.3.1. Spatial Scale Delineation

This study employs two approaches to delineate spatial scale. First, the delineation at the urban agglomeration scale is grounded in national strategic planning. In accordance with key national policy documents, including the *Opinions of the CPC Central Committee and the State Council on Promoting High-Quality Urban Development*, the *Outline of the Plan for Coordinated Development of the Beijing–Tianjin–Hebei Region*, the *Outline of the Regional Integrated Development Plan for the Yangtze River Delta*, and the *Development Plan for the Guangdong–Hong Kong–Macao Greater Bay Area*. This study selects three major urban agglomerations (the BTH, YRD, and GBA) as macro-level analytical units to investigate the spatiotemporal evolution of their ISA. Second, the delineation at the urban scale is based on the city size. Relying exclusively on the aggregate perspective of urban agglomerations may obscure the inherent heterogeneity among their constituent cities. Therefore, to analyze the

developmental patterns of cities across different hierarchical tiers, this study incorporates the dimension of urban scale. In accordance with the *State Council's Notice on Adjusting the Standards for Categorizing City Sizes* and data from the Seventh National Population Census, five megacities-Beijing, Shanghai, Tianjin, Guangzhou, and Shenzhen-were selected from the three major urban agglomerations as representative case studies. Analyzing these five megacities provides an empirical foundation for elucidating the urbanization patterns within China's three major urban agglomerations.

2.3.2. Impervious Surface Expansion Indicators

The impervious surface expansion rate (ISER) is used to quantify the annual net increase in ISA during the study period. In contrast, the impervious surface expansion intensity (ISEI) characterizes the relative rate of spatial change, primarily reflecting the magnitude and degree of impervious surface area changes within the study area over a given timeframe.

The calculation formulas are as follows:

$$\mathrm{ISER} = \frac{(U_b - U_a)}{T} \tag{1}$$

$$\mathrm{ISEI} = \frac{U_b - U_a}{U_a} \times \frac{1}{T} \times 100\% \tag{2}$$

where ISER is the impervious surface expansion rate; ISEI is the impervious surface expansion intensity; U_a and U_b represent the area of the land use type at the beginning and end of the research period (km^2), respectively, and T denotes the time interval (in years) between the two time points. Specifically, if the interval is ten years, T = 10.

By comparing land use data from the beginning and end of the study period, this study constructs a land use transition matrix to reveal the characteristics and dynamic evolution of land use types, thereby facilitating the analysis of changing trends [58]. Derived from the Markov model, the land use transition matrix quantitatively describes the transitions between different land use types, detailing both the extent of the area and the direction of transfer [59].

The calculation formula for the land use transfer matrix is as follows:

$$S_{ij} = \begin{Bmatrix} s_{11} & \cdots & s_{1n} \\ \vdots & \ddots & \vdots \\ s_{n1} & \cdots & s_{nn} \end{Bmatrix} \tag{3}$$

where S_{ij} denotes the area of land use type i converted to land use type j from the beginning to the end of the research period; i and j represent the land use types at the start and end of the research period, respectively; and n is the total number of land use types during the research period.

2.3.3. Identification of Urban Expansion Types

Traditional expansion indices typically focus exclusively on spatial relationships among nearest neighbors, which can introduce biases when characterizing the overall structure of urban expansion. To overcome this limitation, this study adopts a novel index—the LCI—to quantitatively describe the urban expansion process [55]. The centrality of the new patch essentially reflects its proximity to the core areas of old patches. However, old patches often consist of multiple spatially dispersed sub-regions, and each sub-region possesses its own independent centroid. Therefore, when assessing centrality, the spatial relationships between new patches and old patches must be comprehensively evaluated, rather than being limited to one or a few isolated urban centers. In contrast to

traditional expansion indices, which primarily focus on spatial proximity to the nearest patches, the LCI evaluates the location of new patches from a macroscopic, city-wide perspective. Consequently, it effectively captures the overall spatial structure of urban expansion. Its principles are as follows.

In this study, urban expansion is characterized using impervious surface data. First, the acquired multitemporal impervious surface data in raster format were vectorized, retaining all small and isolated patches. Second, treating the vector data from the preceding time point as old patches, the Erase tool in ArcGIS10.4 is utilized to subtract these earlier data from the data of the subsequent time point to delineate new patches. All spatial analyses were performed using a projected coordinate system (e.g., WGS_1984_UTM projection) to ensure accurate area and distance measurements. In total, five megacities were analyzed, each spanning four phases (1985–1995, 1995–2005, 2005–2015, and 2015–2024). Finally, geospatial analysis tools are applied to extract the attributes of both new and old patches—specifically, the area of each new patch and each old patch—to calculate the spatial relationship weights.

The calculation formula for the "area-inverse distance" weighting algorithm is as follows:

$$W_{ij} = \frac{A_j d_{ij}^{-2}}{\sum_{j=1}^{n} A_j d_{ij}^{-2}} \quad (4)$$

where W_{ij} is the spatial relationship weight of the new patch(i) relative to the old patch(j); A_j is the area of the old patch j; and d_{ij} is the minimum distance from the centroid of the new patch i to the boundary of old patch j.

The formula for calculating the LCI is as follows:

$$LCI_i = \sum_{j=1}^{n} \frac{A_j d_{ij}^{-2}}{\sum_{j=1}^{n} A_j d_{ij}^{-2}} \sqrt{\frac{A_j}{\pi}} D_{ij}^{-1} \quad (5)$$

where LCI_i is the location centrality index of the new patch i; n is the total number of old patches; D_{ij} is the distance from the boundary of new patch i to the centroid of old patch j; A_j and d_{ij} are defined as in Equation (4); and the range of LCI is (0, ∞), with a higher value indicating a greater degree of centrality for the new patch (Figure 3a).

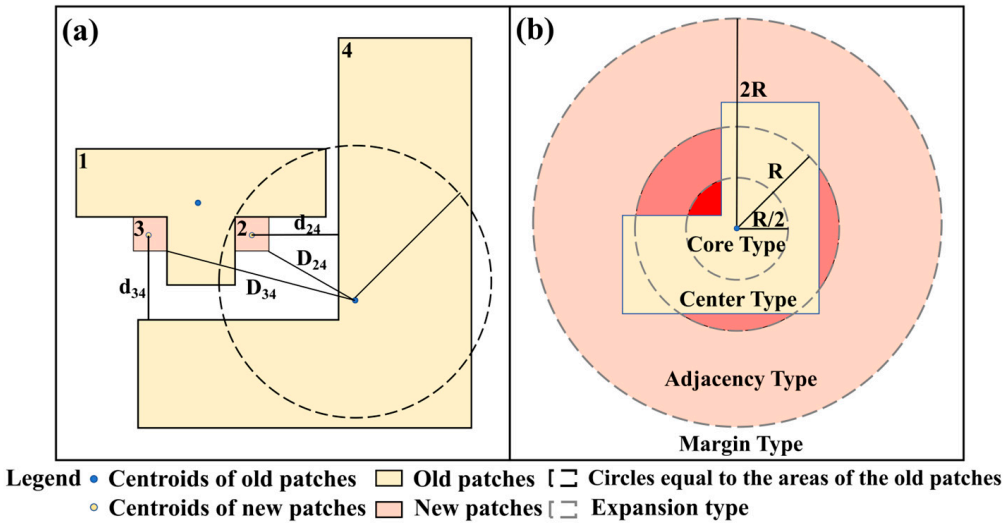


Figure 3. Schematic of the LCI design (**a**) and its spatial centrality classification (**b**).

In this study, an "area-inverse distance" weighting algorithm is employed to calculate the spatial weights between new patches and all old patches, thereby deriving the LCI

for each new patch. Because a circle is the most compact geometric shape, the ratio of the radius of an old patch's equivalent-area circle to the distance from a new patch to the centroid of the old patch can be used to determine the location centrality type. This approach facilitates the identification of expansion types for new patches, thereby revealing their impact on the overall structure of urban expansion [55]. Based on the LCI, urban expansion can be classified into four types: core type, center type, adjacency type, and margin type [55]. The specific criteria for these four types are as follows (Figure 3b). The core type refers to the new patches located extremely close to the centroid of an old patch ($D < R/2$, $LCI > 2$); the center type refers to new patches located relatively close to an old patch ($R/2 \leq D < R$, $1 < LCI \leq 2$); the adjacency type refers to new patches adjacent to an old patch ($R \leq D < 2R$, $0.5 < LCI \leq 1$); and the margin type refers to new patches isolated from an old patch ($2R \leq D$, $0 < LCI \leq 0.5$). The expansion type based on LCI are presented in Table 1.

Table 1. Classification criteria for expansion type based on LCI.

Expansion Type	D Relative to R	LCI
Core type	$D < R/2$	$(2, \infty)$
Center type	$R/2 \leq D < R$	$(1, 2]$
Adjacency type	$R \leq D < 2R$	$(0.5, 1]$
Margin type	$2R \leq D$	$(0, 0.5]$

3. Results

3.1. Spatiotemporal Variations of ISA in China's Three Major Urban Agglomerations

3.1.1. Analysis of Temporal Variations in ISA

Table 2 and Figure 4 illustrate the areal extent and dynamic changes of impervious surfaces across China's three major urban agglomerations from 1985 to 2024. Overall, the total ISA in these regions expanded from 22,544.10 km^2 in 1985 to 69,348.59 km^2 in 2024—a net increase of 46,804.49 km^2—despite a general downward trend in both expansion rate and intensity. Regarding regional characteristics, the BTH urban agglomeration exhibited the largest initial ISA base, reaching 14,702.75 km^2 as early as 1985. Although its expansion rate remained relatively stable throughout the study period, its expansion intensity weakened continuously, declining from 3.21%/a to 1.15%/a. The ISA of the YRD urban agglomeration grew from 6844.85 km^2 in 1985 to 28,683.48 km^2 in 2024, representing an approximately 3.2-fold increase. Its expansion rate peaked at 815.55 km^2/a between 2005 and 2015, with the expansion intensity remaining consistently above 5%/a during the first three periods. The GBA urban agglomeration experienced intense early expansion, with the intensity reaching 13.05%/a between 1985 and 1995. This momentum subsequently slowed significantly, with the expansion intensity dropping to 1.59%/a during the 2015–2024 period, reflecting a development pattern of rapid initial growth followed by steady deceleration. In summary, the development paradigm of these three major urban agglomerations has transitioned from a phase of rapid urbanization driven by incremental expansion and toward an adjacency-dominated, infill-oriented expansion.

Based on the growth scale and expansion intensity of the ISA, the evolutionary trajectories of the three major urban agglomerations can be divided into the following four phases. The first phase (1985–1995): Initial Exploration Phase. During this phase, the ISA began a steady expansion, exhibiting an average annual growth of 0.09×10^4 km^2. Expansion intensity across the urban agglomerations demonstrated a clear spatial gradient, ranked as follows: the GBA (13.05%), the YRD (5.05%), and the BTH (3.21%). Growth in the GBA was particularly prominent, with its expansion intensity reaching a historical peak of 22.17% in 1993. The second phase (1995–2005): Accelerated Expansion Phase. The average annual

ISA expansion rose to 0.13 × 10^4 km^2. The expansion of the YRD urban agglomeration was the most pronounced, with its average annual expansion area and intensity reaching 579.19 km^2 and 5.62%, respectively. In 2004, the expansion intensity of the YRD (8.08%) significantly outpaced that of the BTH (2.14%) and the GBA (5.78%). The third phase (2005–2015): High-speed Development Phase. This phase represented the "golden age" of China's rapid urbanization, with the scale of ISA expansion reaching its zenith at an average annual increase of 0.16 × 10^4 km^2. Expansion rates in the BTH and YRD also peaked simultaneously, with average annual expansion areas reaching 651.76 km^2 and 815.55 km^2, respectively, reflecting the massive scale of urban construction and spatial expansion. The fourth phase (2015–2024): Deceleration and Quality Enhancement Phase. During this phase, the average annual expansion rate moderated to 0.09 × 10^4 km^2, returning to levels comparable to those of the Initial Exploration Phase. Expansion intensity weakened significantly, with all three major urban agglomerations recording intensities below 3%. This shift reflects the transition of the urban development paradigm from incremental expansion to the qualitative enhancement of existing stock.

Table 2. Characteristics of ISA, ISER, and ISEI in China's three major urban agglomerations from 1985 to 2024.

Year *	Phase **	BTH			YRD			GBA		
		ISA (km^2)	ISER (km^2/a)	ISEI (%/a)	ISA (km^2)	ISER (km^2/a)	ISEI (%/a)	ISA (km^2)	ISER (km^2/a)	ISEI (%/a)
1985	-	14,702.75	-	-	6844.85	-	-	996.50	-	-
1995	1985–1995	19,424.53	472.18	3.21	10,304.71	345.99	5.05	2297.03	130.05	13.05
2005	1995–2005	23,819.73	439.52	2.26	16,096.58	579.19	5.62	4702.80	240.58	10.47
2015	2005–2015	30,337.38	651.76	2.74	24,252.12	815.55	5.07	6298.42	159.56	3.39
2024	2015–2024	33,464.04	347.41	1.15	28,683.48	492.37	2.03	7201.07	100.29	1.59

* The ISA indicator corresponds to the "Year" column, ** the ISER and ISEI indicators correspond to the "Phase" column.

3.1.2. Spatial Distribution of ISA

Between 1985 and 2024, the spatial distribution of the ISA across the three major urban agglomerations was characterized by the coexistence of commonalities and differences. Figure 5 illustrates the typical dual-core-driven, radial spatial structure of the BTH. Its ISA distribution is highly uneven and heavily concentrated in the two core cities of Beijing and Tianjin. Regarding expansion morphology, the growth of impervious surfaces displays a distinct radial pattern, extending primarily along major transportation corridors thar connect Beijing and Tianjin to key node cities in Hebei Province, such as Shijiazhuang and Tangshan.

Figure 6 illustrates that the spatial structure of the YRD has undergone an evolutionary transition from a single-core radial pattern to a multi-core networked configuration. The distribution of its ISA has formed a networked layout, with Shanghai serving as the primary hub and major cities such as Nanjing and Hangzhou acting as backbone nodes. Particularly within the Suzhou–Wuxi–Changzhou core region, ISA have coalesced significantly, giving rise to a highly integrated and networked megacity region.

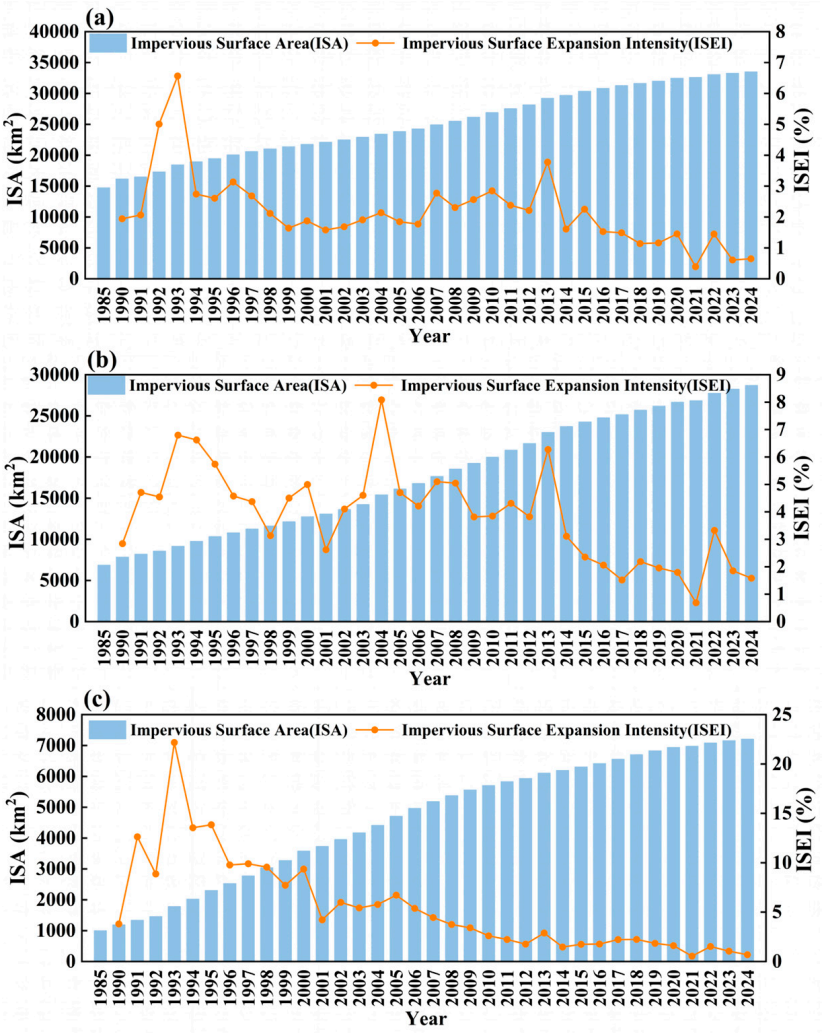


Figure 4. Trends in ISA and ISEI in BTH (**a**), YRD (**b**), and GBA (**c**) from 1985 to 2024.

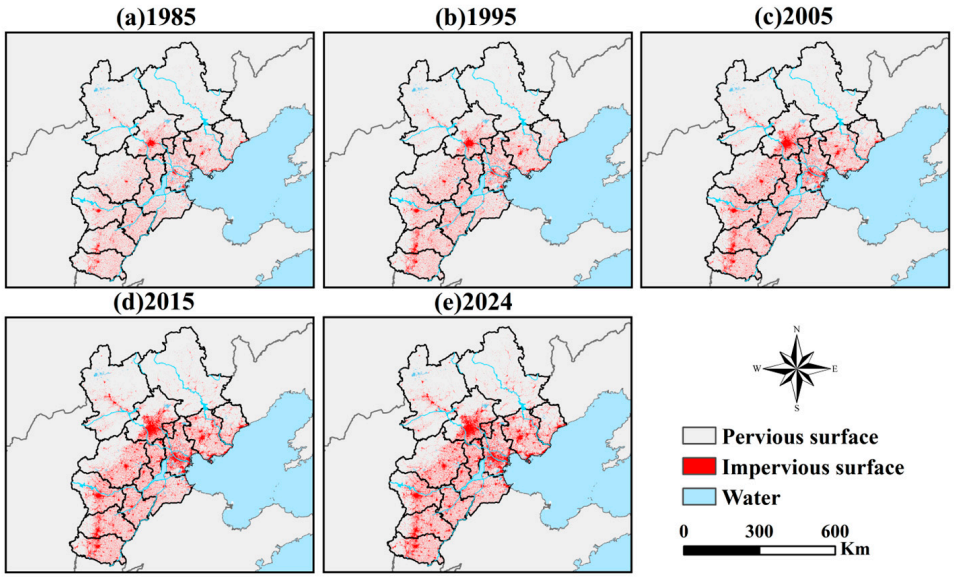


Figure 5. Distribution of ISA in the BTH from 1985 to 2024.

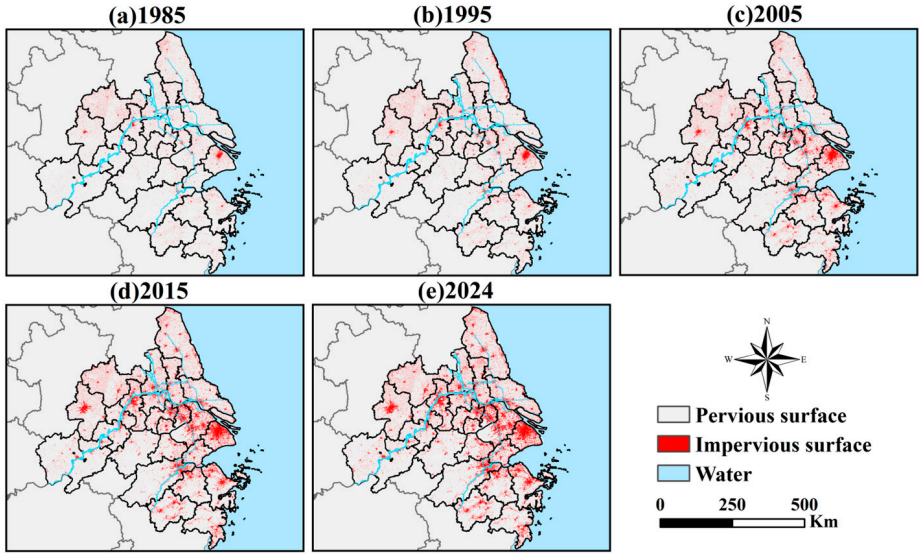


Figure 6. Distribution of ISA in the YRD from 1985 to 2024.

Figure 7 indicates that the ISA within the GBA has increased significantly over the past four decades, characterized by an axial development pattern along the Pearl River and the coastline. Guangzhou and Shenzhen have established high-density clusters on the east and west banks of the Pearl River Estuary, driving the profound integration of cities such as Foshan and Dongguan, and culminating in the formation of two major metropolitan areas: Guangzhou–Foshan–Zhaoqing and Shenzhen–Dongguan–Huizhou. In contrast to the BTH and YRD, the expansion of ISA in the GBA exhibits a pronounced centripetal dynamic and coastal orientation, manifesting as a concentric gradient structure that diminishes outward from the core cities of Guangzhou and Shenzhen toward the periphery.

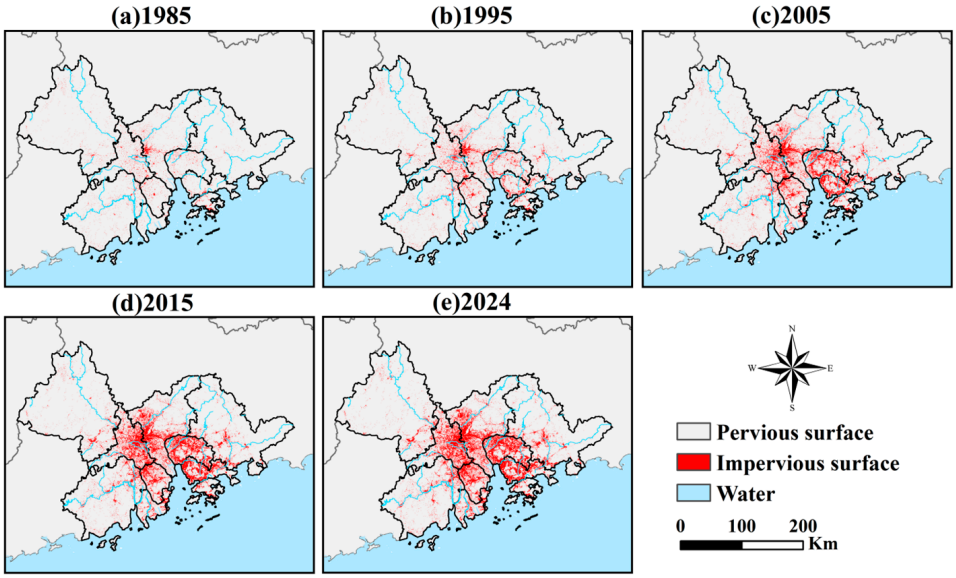


Figure 7. Distribution of ISA in the GBA from 1985 to 2024.

In summary, the spatial distribution patterns of the ISA across the three major urban agglomerations reflect not only their physical geographical foundations but also the projection of diverse regional development models and economic structures onto geographic space. These distinct spatial morphologies provide a crucial empirical lens for understanding the diversity and complexity inherent in China's urbanization.

3.2. Characteristics of ISA Change in Megacities

3.2.1. Spatiotemporal Variation of ISA in Megacities

Figure 8 illustrates the spatial evolutionary trajectories of ISA expansion across the five megacities. Beijing's expansion exhibits a concentric sprawl pattern. While the initial ISA (blue areas) was highly concentrated within the core urban districts, subsequent expansion (orange and red areas) extended outward toward the periphery, primarily along major transportation axes. This is particularly evident in key development zones such as Tongzhou and Yizhuang, which have formed large-scale, spatially contiguous built-up areas. Shanghai's ISA expansion is characterized by multi-nucleated clustering and river-oriented development. While early ISA was densely concentrated along both banks of the Huangpu River, subsequent stages witnessed the emergence of multiple secondary growth poles within the Pudong New Area and various suburban new towns. In contrast, Tianjin's expansion exhibits a strategic, dual-core driven pattern. Alongside the central urban area, the Binhai New Area constitutes a second core growth pole that complements the central city, underscoring its distinctive development trajectory. Guangzhou's expansion is characterized by riverine extension and multi-point dispersal. Early expansion was primarily distributed along the Pearl River and the city's major axes, whereas later stages saw the formation of several new growth nodes in peripheral areas such as Huangpu, Baiyun, and Nansha. Shenzhen's spatial morphology is the most compact, with its ISA reaching a high-density state during its early development. In later periods, constrained by limited land resources and geographical conditions, newly added ISA patches became relatively fragmented; expansion was primarily characterized by the infilling of internal gaps within existing built-up areas and limited outward extension toward peripheral regions such as Bao'an and Longgang.

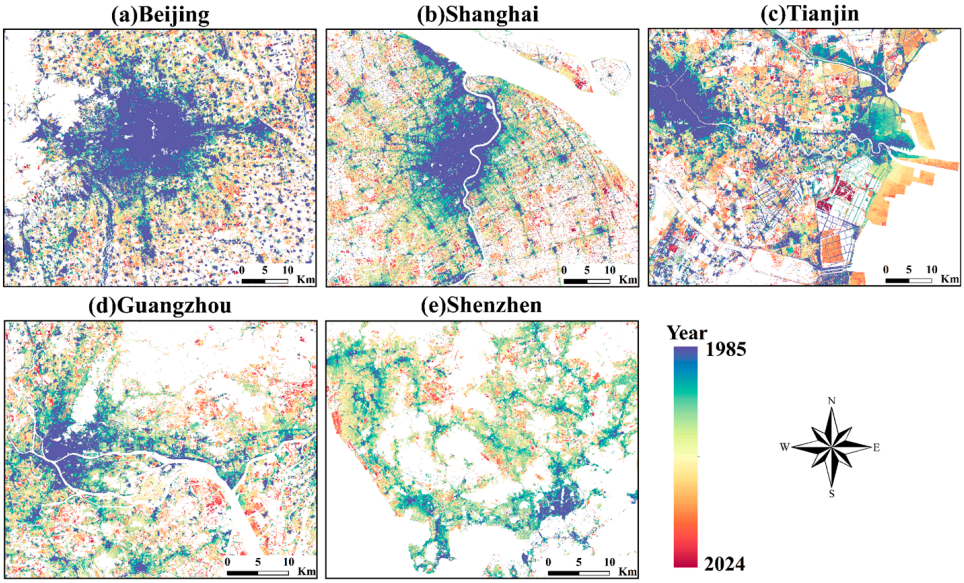


Figure 8. Temporal and spatial changes in annual growth of ISA in the urban cores of Beijing (**a**), Shanghai (**b**), Tianjin (**c**), Guangzhou (**d**), and Shenzhen (**e**) from 1985 to 2024.

Table 3 presents the characteristics of ISA expansion across the five megacities from 1985 to 2024. Overall, while all five cities experienced sustained and rapid urbanization, significant disparities existed in their expansion rates, intensities, and phased growth patterns. Beijing, Shanghai, and Tianjin demonstrated a continuous expansion trend throughout the study period. Notably, Tianjin's average annual expansion rate reached 99.74 km^2/a between 2005 and 2015, ranking among the highest nationwide during this period and highlighting its robust spatial growth momentum. Concurrently, Beijing and

Shanghai recorded average annual expansion rates of 71.45 km^2/a and 60.28 km^2/a, respectively, underscoring their sustained spatial growth trajectories.

Table 3. Characteristics of ISER and ISEI from 1985 to 2024 in Beijing, Shanghai, Tianjin, Guangzhou, and Shenzhen.

City	1985–1995		1995–2005		2005–2015		2015–2024	
	ISER (km^2/a)	ISEI (%/a)	ISER (km^2/a)	ISEI (%/a)	ISER (km^2/a)	ISEI (%/a)	ISER (km^2/a)	ISEI (%/a)
Beijing	43.12	0.27	72.41	0.36	71.45	0.26	18.63	0.06
Shanghai	36.36	0.56	72.53	0.71	60.28	0.35	31.93	0.15
Tianjin	58.97	0.35	54.45	0.24	99.74	0.35	35.21	0.10
Guangzhou	23.88	1.04	44.69	0.96	30.15	0.33	18.00	0.16
Shenzhen	18.48	3.69	35.59	1.52	13.53	0.23	4.46	0.07

In contrast, the average annual expansion areas of Guangzhou and Shenzhen are smaller, primarily attributable to the smaller initial baseline sizes of their built-up areas. The development trajectory of Shenzhen, as a quintessential emerging megacity, is particularly noteworthy. Between 1985 and 1995, despite an absolute expansion rate of only 18.48 km^2/a, its expansion intensity reached a striking 3.69%/a. This explosive growth underscores the rapid spatial expansion that occurred during the early establishment of the Special Economic Zone. Subsequently, its expansion intensity gradually decelerated, the expansion rate stabilized at 35.59 km^2/a during the 1995–2005 period, while the intensity remained relatively high at 1.52%/a. This suggests that the extreme intensity of early-stage land development in Shenzhen led to rapid urban spatial saturation. Guangzhou similarly exhibited characteristics of high early-stage growth, with expansion intensities reaching 1.04%/a and 0.96%/a during the 1985–1995 and 1995–2005 periods, respectively. Concurrently, its absolute expansion rate demonstrated a strong and persistent upward trend, rising from 23.88 km^2/a in 1985–1995 to 44.69 km^2/a in 1995–2005, an increase of nearly 87%. This indicates a more prolonged high-speed expansion cycle, underscoring Guangzhou's status as the central city of South China.

3.2.2. Land Use Impacts of Impervious Surface Expansion

The results of the land use transition matrix analysis presented in Figure 9 indicate that between 1985 and 2024, the land use structures of the five megacities underwent transformations characterized primarily by impervious surface area expansion and cropland reduction. Cropland served as the predominant land source for this expansion, although the evolutionary trajectories and patterns of each city exhibited distinct regional heterogeneity. Beijing's development pattern is defined by the simultaneous progression of impervious surface area expansion and ecological conservation. During the study period, its cropland area decreased significantly from 2828.56 km^2 to 1765.86 km^2, while the ISA surged from 676.58 km^2 to 1539.07 km^2. Meanwhile, the forest area grew steadily, rising from 2995.56 km^2 to 3368.12 km^2. In Shanghai, land use change was predominantly concentrated in the large-scale conversion of cropland to impervious surface areas. The city's cropland area plummeted from 5685.73 km^2 to 4055.05 km^2, while its ISA concurrently surged from 655.05 km^2 to 2634.16 km^2. This dynamic reflects the rapid urbanization of the Pudong New Area and stands in stark contrast to the pattern observed in Beijing.

Compared to their northern cities, the southern cities, exemplified by Guangzhou and Shenzhen, have expanded more rapidly. Guangzhou's land use pattern is characterized by the concurrent conversion of cropland to impervious and the preservation of high forest coverage, and impervious surface area expanded rapidly, with their area surging from 221.62 km^2 to 1335.41 km^2, representing a more than fivefold increase. Guangzhou's forest

area has consistently remained at approximately 3000 km^2, benefiting from the city's favorable natural endowments. Among the five cities, Shenzhen exhibits the most pronounced rate and intensity of land use transformation. Its ISA underwent explosive growth, rising from 185.42 km^2 to 2835.86 km^2 and encroaching extensively upon both cropland and forest. Consequently, its cropland area plummeted from 2591.67 km^2 to 1288.56 km^2, while the forest area decreased from 3709.55 km^2 to 2665.58 km^2. Shenzhen's evolutionary trajectory is defined by high-intensity land conversion, reflecting the "land-for-development" model prevalent across most Chinese cities during the era of rapid urbanization.

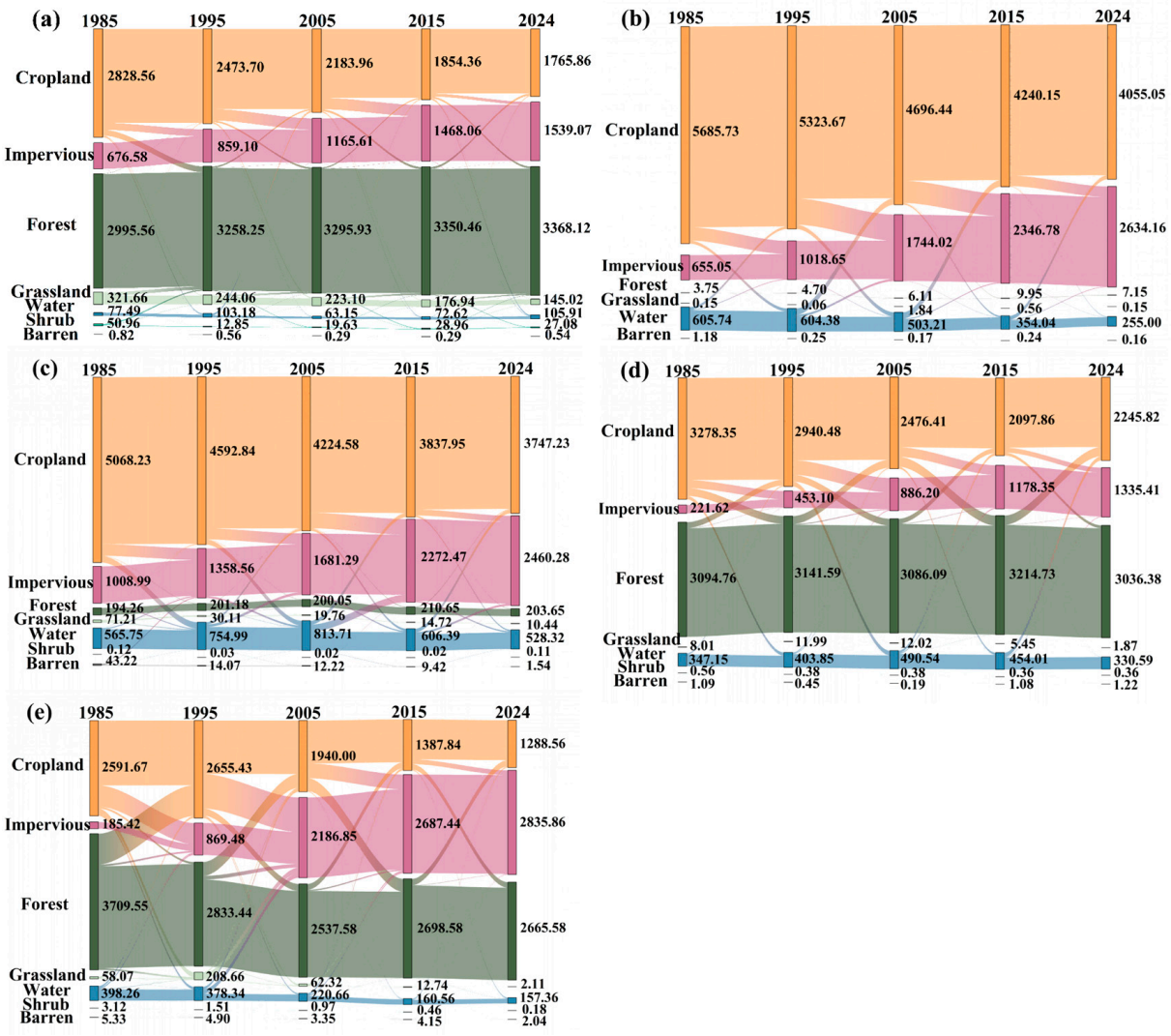


Figure 9. Land use changes (km^2) in Beijing (**a**), Shanghai (**b**), Tianjin (**c**), Guangzhou (**d**), and Shenzhen (**e**) from 1985 to 2024.

3.3. Analysis of Urban Expansion in Megacities

Urban expansion represents the most direct spatial manifestation of urbanization. This study examines the spatial expansion patterns within the core urban areas of five major megacities, Beijing, Shanghai, Tianjin, Guangzhou, and Shenzhen. The research utilizes the LCI to classify newly expanded impervious surface area into four expansion types: Core, Center, Adjacency, and Margin. By analyzing the temporal variations in the proportions of these expansion types, this study elucidates the evolutionary trajectories and structural characteristics of spatial expansion across these cities.

As shown in Table 4, compared to Initial Exploration Phase (1985–1995), a common characteristic of the five megacities in the Deceleration and Quality Enhancement Phase

(2015–2024) is that the proportion of adjacency expansion type shows a significantly increasing trend, while the proportion of margin expansion type exhibits a decreasing trend. Among them, adjacency expansion type has become the dominant form, exceeding 50% in most cities. This indicates that urban expansion is increasingly characterized by infilling and contiguous development along the fringes of existing built-up areas. However, in terms of the combined proportion of the core and center expansion types, the expansion processes of the five megacities demonstrate distinct divergence. The changes in Beijing, Shanghai, and Tianjin are relatively stable, with Tianjin showing a slight increase, whereas Guangzhou and Shenzhen present a highly significant decline. Consequently, in the subsequent analysis, Beijing, Shanghai, and Tianjin will be analyzed together, while Guangzhou and Shenzhen will be analyzed as another.

Table 4. Statistics of the patches according to different expansion type based on LCI values.

City	Expansion Type	1985–1995		1995–2005		2005–2015		2015–2024	
		Area (km^2)	Proportion (%)	Area (km^2)	Proportion (%)	Area (km^2)	Proportion (%)	Area (km^2)	Proportion (%)
Beijing	Core	20.85	8.85	31.64	8.21	25.55	6.99	3.42	3.93
	Center	87.42	37.09	132.07	34.27	117.31	32.11	37.03	42.61
	Adjacency	111.22	47.19	207.61	53.88	217.48	59.54	45.85	52.77
	Margin	16.21	6.88	14.03	3.64	4.97	1.36	0.60	0.69
Shanghai	Core	29.82	13.13	42.05	9.63	29.90	8.26	12.85	9.06
	center	64.84	28.55	114.04	26.11	100.12	27.66	42.16	29.72
	Adjacency	99.71	43.91	191.26	43.79	209.67	57.92	81.79	57.66
	Margin	32.72	14.41	89.44	20.48	22.33	6.17	5.06	3.57
Tianjin	Core	60.04	24.07	38.62	14.55	90.89	19.18	26.36	16.28
	center	74.21	29.75	76.53	28.83	108.33	22.86	73.41	45.32
	Adjacency	79.18	31.74	121.37	45.73	263.02	55.50	61.32	37.86
	Margin	36.04	14.45	28.92	10.89	11.65	2.46	0.88	0.54
Guangzhou	Core	15.74	13.68	33.95	17.04	13.33	10.09	4.62	8.15
	center	37.16	32.31	50.45	25.33	27.77	21.03	9.75	17.20
	Adjacency	33.70	29.30	65.92	33.09	65.15	49.33	31.56	55.72
	Margin	28.41	24.70	48.89	24.54	25.80	19.54	10.72	18.93
Shenzhen	Core	56.78	40.92	90.21	35.87	7.33	7.36	2.00	7.23
	center	33.27	23.98	79.19	31.49	23.05	23.15	9.76	35.27
	Adjacency	9.97	7.18	56.27	22.37	59.28	59.53	15.06	54.39
	Margin	38.75	27.92	25.83	10.27	9.91	9.95	0.86	3.11

Compared to the Initial Exploration Phase (1985–1995), the combined proportion of core and center expansion types during the Deceleration and Quality Enhancement Phase (2015–2024) remained relatively stable in Beijing, Shanghai, and Tianjin, with Tianjin exhibiting a marginal increase (Figure 10). Regarding expansion patterns, the expansion of adjacency type has long maintained a dominant position, while the expansion of center type has also been continuously reinforced. Between 2015 and 2024, the proportions of adjacency type in Beijing, Shanghai, and Tianjin reached 52.77%, 57.66%, and 37.86%, respectively. Concurrently, as urban central functions continued to strengthen, the proportion of center type rose significantly, reaching 42.61%, 29.72%, and 45.32% in Beijing, Shanghai, and Tianjin, respectively. Meanwhile, the proportion of margin expansion in these three cities dropped to exceptionally low levels during the 2015–2024 period, recorded at 0.69%, 3.57%, and 0.54%, respectively. Notably, the combined proportion of core and center type in Tianjin exceeded 60% during the 2015–2024 period, ranking first among the five megacities and surpassing both Beijing and Shanghai. Tianjin has successfully transitioned from monocentric expansion to a dual-core intensive structure, with newly expanded

areas primarily concentrated in the Binhai New Area and the "Ecological-Development Composite Corridor" connecting the two urban centers.

Compared to Phase 1 (1985–1995), the combined proportion of core and central types in Guangzhou and Shenzhen exhibited a significant decline during Phase 4 (2015–2024). The core cities of the GBA, represented by Guangzhou and Shenzhen, underwent significant spatial restructuring prior to 2005 (Figure 11). During the early phases, their expansion patterns were primarily characterized by large-scale, extensive development, manifesting as multiple dispersed core and center expansion types. Between 1985 and 1995, the proportions of margin type in Shenzhen and Guangzhou were 27.92% and 24.70%, respectively, significantly higher than those of Tianjin (14.45%), Shanghai (14.41%), and Beijing (6.88%) during the same period. From 1995 to 2005, the proportion of Margin type in Shenzhen dropped from 27.92% to 10.27%, whereas in Guangzhou, it only decreased marginally from 24.70% to 24.54%. This indicates that land development had not yet formed a highly intensive concentric structure during the rapid takeoff of urbanization. Meanwhile, core and center types occupied prominent positions in both Guangzhou and Shenzhen. Between 1985 and 1995, the core and center expansion types in Shenzhen accounted for 40.92% and 23.98%, respectively, while the corresponding proportions for Guangzhou were 13.68% and 32.31%. This "dual-high" pattern of core and margin expansion types suggests that both cities were in a transitional development stage characterized by the coexistence of high-intensity urban core development and peripheral sprawl. Consequently, their spatial compactness was significantly lower than that of megacities such as Beijing and Shanghai. After 2005, adjacency expansion type emerged as the dominant mode for both cities. During the 2015–2024 period, the proportions of adjacency expansion type in Guangzhou and Shenzhen reached as high as 55.72% and 54.39%, respectively. However, the two cities exhibited divergent characteristics regarding center and margin expansion types. In Guangzhou, the proportion of center expansion type decreased from 21.03% in the 2005–2015 period to 17.20% in the 2015–2024 period. Meanwhile, its proportion of margin expansion type remained high at 18.93% during 2015–2024, maintaining a persistently elevated level that significantly exceeded those of the other four megacities. In contrast, the proportion of center expansion type in Shenzhen rose substantially to 35.27%, while its proportion of margin expansion type plummeted to 3.11%, marking the most significant decline among the five megacities. These results suggest that, despite the emergence of multiple growth poles during its development, Guangzhou has not effectively consolidated them into cohesive and spatially compact urban cores. Conversely, over the past four decades, Shenzhen has undergone significant spatial restructuring, shifting from extensive sprawl toward intensification and achieving a transition from dispersed, large-scale expansion to more concentrated development.

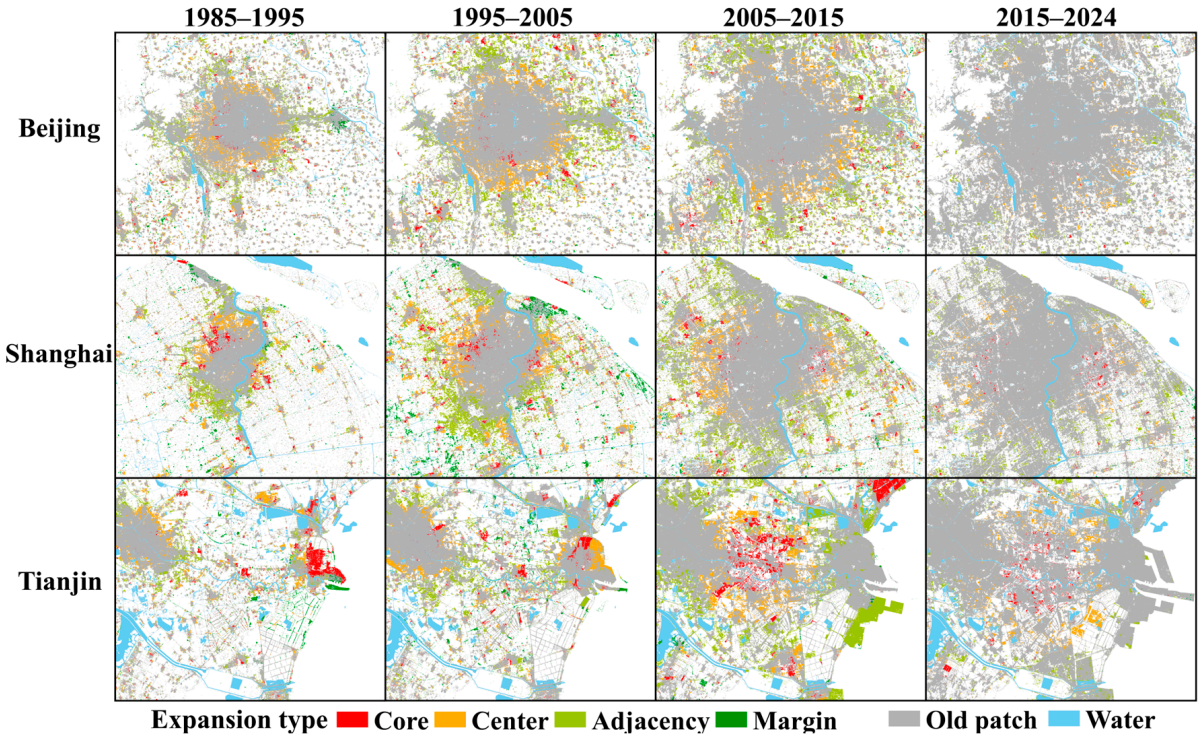


Figure 10. Spatial distribution of different expansion type based on LCI values in the urban cores of Beijing, Shanghai, Tianjin from 1985 to 2024.

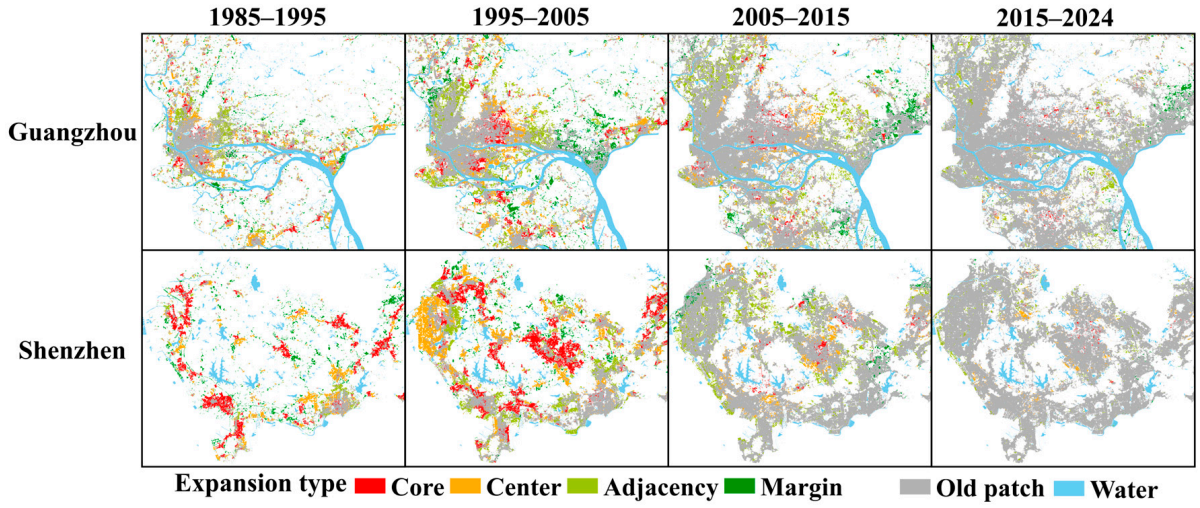


Figure 11. Spatial distribution of different expansion type based on LCI values in the urban cores of Guangzhou, Shenzhen from 1985 to 2024.

4. Discussion

4.1. Comparison with Previous Studies

Based on long-term CLCD data, this study comprehensively analyzes the evolutionary characteristics of ISA and urban expansion across three major urban agglomerations. The results indicate that over the past 40 years, although the ISA in these regions has grown continuously, the rate and intensity of expansion have generally exhibited a decelerating trend, aligning with existing research on the deceleration of urban expansion in China [57]. Furthermore, in contrast to the three-phase trajectory of urban land evolution in China [60], this study further subdivides the evolution of these agglomerations into four phases based on impervious surface area growth: Initial Exploration Phase (1985–1995), Accelerated

Expansion Phase (1995–2005), High-speed Development Phase (2005–2015), and Deceleration and Quality Enhancement Phase (2015–2024). The research also highlights significant regional differences in peak expansion phases. Specifically, the expansion peak for the GBA occurred during the Initial Exploration Phase (1985–1995), whereas the peaks for the YRD and BTH were concentrated in the High-speed Development Phase (2005–2015).

This research further focuses on the urban agglomeration and megacity scales, providing a comprehensive and systematic analysis of impervious surface evolution across multidimensional spatial scales. Regarding the spatial characteristics of ISA within urban agglomerations, the distribution in the BTH region is highly uneven, being heavily concentrated in the core cities of Beijing and Tianjin. In contrast, the YRD and GBA exhibit distinct agglomeration characteristics and a more balanced distribution, which is entirely consistent with conclusions derived from long-term nighttime light datasets [61]. At the city scales, rapid urbanization has driven the conversion of large areas of natural surfaces into impervious surfaces, with the most profound impact on cropland [38]. The encroachment of impervious surfaces upon ecological land has exacerbated the fragmentation of urban ecosystems. Based on the land use transition matrix, the land use of Beijing, Shanghai, Tianjin, Guangzhou, and Shenzhen over the past 40 years have been consistently characterized by the expansion of impervious surfaces and the shrinkage of cropland. Data regarding land use conversion mode ratios from 1984 to 2024 in China indicate that cropland and bare land serve as the primary sources for urban expansion [60]. Among the studied cities, Shenzhen has experienced the most drastic land use evolution, with its rural landscape being almost entirely replaced by urban land by 2020 [60]. This study further quantifies these changes, revealing that the ISA in Shenzhen surged from 185.42 km^2 in 1985 to 2835.86 km^2 in 2024, while the areas of forest and cropland plummeted from 3709.55 km^2 and 2591.67 km^2 to 2665.58 km^2 and 1288.56 km^2, respectively. In terms of quantitatively characterizing urban expansion, Liu et al. analyzed the expansion structure of the Wuhan Metropolitan Area using the LCI, demonstrating its applicability in identifying urban expansion patterns [55]. The present study extends the application of the LCI to five megacities, including Beijing and Shanghai. The results indicate that the urban expansion of these five megacities was dominated by adjacency expansion type from 1985 to 2024. This characteristic may be closely related to their urban scale, further validating the significant advantages of the LCI in identifying and describing urban expansion patterns and their evolutionary trajectories.

4.2. Limitations and Future Work

This research provides the first systematic monitoring of dynamic changes in ISA across China's three major urban agglomerations over the past four decades, offering a novel perspective on large-scale land use evolution. However, the study has certain limitations. First, regarding data selection and continuity, rather than utilizing dedicated impervious surface datasets such as GAIA, this research opted to extract ISA data from the CLCD dataset to leverage its longer time series, although Chen et al. similarly used ISA data derived from the CLCD [57]. Most notably, the extracted ISA data include certain rural areas, which may influence the analytical results. Second, our analysis relies on policy-based boundaries for urban agglomerations. We acknowledge that alternative delineations-such as those based on functional linkages (e.g., commuting flows) or ecological continuity-might capture different dimensions of urban expansion and could lead to variations in the specific results. Third, this study has not yet conducted a quantitative analysis of the driving factors behind impervious surface area expansion, such as policy, economy, population growth, and infrastructure. These limitations warrant further investigation in future research.

From a methodological perspective, although this study does not quantitatively compare the LCI with traditional methods such as the landscape expansion index, a theoretical discussion of their relative advantages and disadvantages helps us to understand the applicability of the LCI. In contrast to traditional expansion indices, which primarily focus on spatial proximity to the nearest patches, the LCI evaluates the location of new patches from a macroscopic, city-wide perspective. Consequently, it effectively captures the overall spatial structure of urban expansion. By employing the "area-inverse distance" weighting algorithm, the LCI comprehensively identifies the centrality of new patches compared with the locations of the main center, subcenter, or potential center [55]. This approach eliminates the subjectivity inherent in parameter settings, compensating for the limitation of traditional indices that focus exclusively on localized expansion patterns while neglecting overall structural characteristics [53,62]. Nevertheless, the LCI has certain limitations. The LCI primarily evaluates the centrality of new patches relative to the overall urban structure, rather than focusing on localized expansion. Since the LCI uses the centroids of old patches as their centers and calculates based on the distance from the boundary of the new patch to these centroids, it may overlook the impact of patch shape.

In summary, the dynamics of impervious surface area expansion revealed in this study provide a scientific basis for urban agglomerations and similar megacities to formulate differentiated spatial management and resilience enhancement strategies. First, regarding spatial planning and management, for areas dominated by margin expansion, it is recommended to strictly delineate urban development boundaries, prioritize guiding newly added construction land toward infill development within or around existing built-up areas, and strictly restrict disorderly leapfrog sprawl. For cities characterized by dual-core or multi-core structures, such as Beijing and Tianjin, ecological buffer zones or green corridors can be designated between core areas based on the urban expansion types identified by the LCI, thereby preventing excessive contiguous urban expansion that exacerbates ecosystem fragmentation. Second, in terms of resilient infrastructure and flood risk prevention, the proportion of green spaces and permeable pavements within core type expansion areas should be moderately increased to mitigate the urban heat island effect and facilitate stormwater infiltration. For margin type expansion areas, stormwater retention and detention facilities should be proactively planned in conjunction with existing hydrological systems and topography. Furthermore, it is recommended to overlay the spatial distribution of impervious surface area expansion with flood inundation risk zoning. In high flood risk areas, the total extent of impervious surfaces should be strictly controlled, mandatory stormwater retention and detention measures must be enforced, and new projects must fully comply with Low-Impact Development management.

5. Conclusions

This study comprehensively evaluated the ISA of China's three major urban agglomerations and the expansion patterns of representative cities from 1985 to 2024. By utilizing impervious surface expansion indicators, this study revealed the spatiotemporal dynamics of impervious surface area and further applied the LCI to investigate the expansion structure and pattern of five megacities. The results indicate that the total ISA of China's three major urban agglomerations expanded from 22,544.10 km^2 to 69,348.59 km^2 from 1985 to 2024. However, both the expansion rate and intensity exhibited a distinct decelerating trend. This shift signifies a fundamental transition in the development paradigm, moving away from rapid urbanization driven by incremental expansion and toward an adjacency-dominated, infill-oriented expansion. However, significant regional variation exists regarding the peak expansion phases. The GBA peaked during the Initial Exploratory Phase (1985–1995), with its ISEI reaching a historical peak of 22.17% in 1993. In contrast, the

YRD and BTH reached their peaks during the High-speed Development Phase (2005–2015), with their ISER reaching 651.76 km^2/a and 815.55 km^2/a, respectively. At the city scale, the LCI-based analysis of urban expansion across five megacities reveals that adjacency expansion type has become the predominant form of growth, exceeding 50% in most cities. This signifies a clear shift toward infill and contiguous development anchored to the peripheries of existing built-up areas. These findings enhance our understanding of the evolutionary trajectories of ISA within urban agglomerations and the expansion patterns of megacities, holding great significance for formulating context-specific urban planning policies and enhancing the resilience of urban development. However, it should be noted that the ISA data extracted in this study include certain rural areas, which may influence the analytical results. This issue warrants further investigation in future research.

Author Contributions: Conceptualization, F.W. and Y.Y.; methodology, F.W.; software, F.W.; validation, F.W.; formal analysis, F.W.; investigation, F.W. and Y.Y.; resources, F.W.; data curation, F.W.; writing—original draft preparation, F.W. and Y.Y.; writing—review and editing, Y.C. and S.Y.; visualization, F.W.; supervision, L.Y. and F.S.; project administration, F.W.; funding acquisition, F.W. All authors have read and agreed to the published version of the manuscript.

Funding: This research was funded by the S&T Innovation and Development Project of Information Institution of Ministry of Emergency Management (Project No. 2024506).

Data Availability Statement: The data source has been declared in the article; further inquiries can be directed to the corresponding author.

Acknowledgments: The authors appreciate the valuable comments from the editor and reviewers.

Conflicts of Interest: The authors declare no conflicts of interest.

Abbreviations

The following abbreviations are used in this manuscript:

ISA	Impervious Surface Area
ISER	Impervious Surface Expansion Rate
ISEI	Impervious Surface Expansion Intensity
BTH	Beijing–Tianjin–Hebei Urban Agglomeration
YRD	Yangtze River Delta Urban Agglomeration
GBA	Guangdong–Hong Kong–Macao Greater Bay Area Urban Agglomeration
LCI	Location Centrality Index
LULC	Land Use/Land Cover
GEE	Google Earth Engine

References

1. Fu, Y.; Mao, Y.; Wu, G. Event-based evaluation of urbanization impact on precipitation during the 1978–2021 warm season over eastern China. *Urban Clim.* **2024**, *56*, 102048. [CrossRef]
2. NBS. Significant Improvement in Urbanization Level and a Brand-New Look of Cities—The 11th Report on Economic and Social Development Achievements in the 40 Years of Reform and Opening Up [EB/OL]. Available online: https://www.stats.gov.cn/zt_18555/ztfx/ggkf40n/202302/t20230209_1902591.html (accessed on 10 September 2018).
3. NBS. Social Services Achieve Positive Development and People's Livelihoods Continuously Improve—A Statistical Report on Social Livelihood Since the 14th Five-Year Plan [EB/OL]. Available online: https://www.stats.gov.cn/xxgk/sjfb/zxfb2020/202509/t20250928_1961404.html (accessed on 28 September 2025).
4. Yang, J.; Wu, T.; Gong, P. Implementation of China's new urbanization strategy requires new thinking. *Sci. Bull.* **2017**, *62*, 81–82. [CrossRef]
5. Fang, C.; Yu, D. Urban agglomeration: An evolving concept of an emerging phenomenon. *Landsc. Urban Plan.* **2017**, *162*, 126–136. [CrossRef]

6. The State Council. Opinions of the Central Committee of the Communist Party of China and the State Council on Promoting High-Quality Urban Development [EB/OL]. Available online: https://www.gov.cn/gongbao/2025/issue_12266/202509/content_7039600.html (accessed on 15 August 2025).
7. Xinhua News Agency. Beijing-Tianjin-Hebei Region's Total Economic Output Crosses Three Trillion-Yuan Thresholds in Five Years [EB/OL]. Available online: https://www.gov.cn/lianbo/202602/content_7059064.htm (accessed on 24 February 2026).
8. NDRC. Development Plan for the Yangtze River Delta Urban Agglomeration [EB/OL]. Available online: https://www.ndrc.gov.cn/xxgk/zcfb/tz/201606/W020190905517021091604.pdf (accessed on 1 June 2016).
9. Guangdong-Hong Kong-Macao Greater Bay Area. About the Guangdong-Hong Kong-Macao Greater Bay Area [EB/OL]. Available online: https://www.cnbayarea.org.cn/introduction/content/post_165071.html (accessed on 12 December 2025).
10. NBS. Statistical Charts on Economic and Social Development: Main Economic Indicators of the Beijing-Tianjin-Hebei Region, the Yangtze River Economic Belt, and the Yangtze River Delta in 2024 [EB/OL]. Available online: https://www.qstheory.cn/20250714/2e946fd2b0854960817f0c1f958f8803/c.html (accessed on 16 July 2025).
11. Guangdong-Hong Kong-Macao Greater Bay Area. Six Sets of Data Show New Development Achievements of the Greater Bay Area in 2024 [EB/OL]. Available online: https://www.cnbayarea.org.cn/news/special/numbers/content/post_1283909.html (accessed on 28 February 2025).
12. Tang, L.; Lan, T.; Xing, X.; Xie, T.; Li, W.; Fang, C.; Cao, Y.; Xu, Y.; Chen, D.; Wang, L.; et al. Past Achievements and Future Strategies of Eco-environmental Construction in Mega Urban Agglomerations in Eastern China. *Bull. Chin. Acad. Sci.* **2023**, *38*, 394–406.
13. Liu, Z.; Xu, X.; Liu, X. Multi-scale determinants of net primary productivity in China's urban agglomerations. *J. Environ. Manag.* **2026**, *404*, 129268. [CrossRef]
14. Ye, H.; Zheng, D.; Leng, B.; Cai, Y.; Zhao, H. Identifying spatial boundary of urban agglomerations and metropolitan areas in China by multi-scale integrated framework. *Cities* **2026**, *173*, 106896. [CrossRef]
15. Zhang, A.; Han, Z.; Sun, G.; Chen, X.; Cheng, J.; Zhang, H. An impervious surfaces extraction method based on optical, ascending and descending SAR remote sensing imagery in high-density urban core areas. *Int. J. Appl. Earth Obs. Geoinf.* **2025**, *140*, 104595. [CrossRef]
16. Dermosinoglou, A.; Petropoulos, G.P. Exploring long term Impervious Surface Areas (ISA) dynamics using Landsat imagery, Machine Learning and GEE: The case of Attica, Greece. *Remote Sens. Appl. Soc. Environ.* **2024**, *36*, 101338. [CrossRef]
17. Ma, Q.; He, C.; Wu, J. Behind the rapid expansion of urban impervious surfaces in China: Major influencing factors revealed by a hierarchical multiscale analysis. *Land Use Policy* **2016**, *59*, 434–445. [CrossRef]
18. Zhang, Y.; Zhu, Y.; Yang, K.; Du, S.; Wang, Q.; Zhao, L.; Peng, Z.; Luo, Y. The response mechanism of urban precipitation to impervious surface expansion. *J. Hydrol. Reg. Stud.* **2025**, *62*, 102789. [CrossRef]
19. Zhang, L.; Zhang, M.; Yao, Y. Mapping seasonal impervious surface dynamics in Wuhan urban agglomeration, China from 2000 to 2016. *Int. J. Appl. Earth Obs. Geoinf.* **2018**, *70*, 51–61. [CrossRef]
20. Zhang, D.; Peng, J.; Yang, Z. Identifying urban agglomeration's range: Integrating clustering and accessibility analysis. *Cities* **2026**, *171*, 106708. [CrossRef]
21. Xu, J.; Zhao, Y.; Sun, C.; Liang, H.; Yang, J.; Zhong, K.; Li, Y.; Liu, X. Exploring the Variation Trend of Urban Expansion, Land Surface Temperature, and Ecological Quality and Their Interrelationships in Guangzhou, China, from 1987 to 2019. *Remote Sens.* **2021**, *13*, 1019. [CrossRef]
22. Man, W.; Nie, Q.; Li, Z.; Li, H.; Wu, X. Using fractals and multifractals to characterize the spatiotemporal pattern of impervious surfaces in a coastal city: Xiamen, China. *Physica A* **2019**, *520*, 44–53. [CrossRef]
23. Zhang, J.; Du, J.; Fang, S.; Sheng, Z.; Zhang, Y.; Sun, B.; Mao, J.; Li, L. Dynamic Changes, Spatiotemporal Differences, and Ecological Effects of Impervious Surfaces in the Yellow River Basin, 1986–2020. *Remote Sens.* **2023**, *15*, 268. [CrossRef]
24. Zhao, C.; Zhang, H.; Wang, H.; Zhao, J. Analysis of changes in the spatiotemporal characteristics of impervious surfaces and their influencing factors in the Central Plains Urban Agglomeration of China from 2000 to 2018. *Heliyon* **2023**, *9*, e18849. [CrossRef] [PubMed]
25. Xiao, C.; Yue, Z.; Feng, Z.; Wang, Y.; Peñuelas, J.; Wu, C. Impervious surface increase over global border areas regulated by population and topography. *Sci. Bull.* **2026**, *71*, 1450–1460. [CrossRef]
26. Xu, S.-C.; Miao, Y.-M.; Gao, C.; Long, R.-Y.; Chen, H.; Zhao, B.; Wang, S.-X. Regional differences in impacts of economic growth and urbanization on air pollutants in China based on provincial panel estimation. *J. Clean. Prod.* **2019**, *208*, 340–352. [CrossRef]
27. Santhanam, H.; Majumdar, R. Quantification of green-blue ratios, impervious surface area and pace of urbanisation for sustainable management of urban lake—Land zones in India—A case study from Bengaluru city. *J. Urban Manag.* **2022**, *11*, 310–320.
28. Huang, X.; Li, F.; Wu, J.; Liu, W.; Wang, F.; Zhang, Z.; Tang, L.; Zhang, X. Spatiotemporal Dynamics and Driving Forces of Impervious Surfaces in Zhengzhou Metropolitan Area [J/OL]. *J. North China Univ. Water Resour. Electr. Power (Nat. Sci. Ed.)* **2025**. Available online: https://link.cnki.net/urlid/41.1432.TV.20250618.1250.002 (accessed on 30 June 2026).

29. Zhang, N.; Ye, H.; Wang, M.; Li, Z.; Li, S.; Li, Y. Response Relationship between the Regional Thermal Environment and Urban Forms during Rapid Urbanization (2000–2010–2020): A Case Study of Three Urban Agglomerations in China. *Remote Sens.* **2022**, *14*, 3749. [CrossRef]
30. Zhu, H.; Li, Y.; Liu, Z.; Fu, B. Estimating the Population Distribution in a County Area in China Based on Impervious Surfaces. *Photogramm. Eng. Remote Sens.* **2015**, *81*, 155–163. [CrossRef]
31. Wang, W.; Bai, X.; Zhang, Y.; Li, L. Spatiotemporal patterns and influencing factors in intercity travel within urban agglomerations. *Transp. Policy* **2026**, *181*, 104024. [CrossRef]
32. Fu, B.; Peng, Y.; Zhao, J.; Wu, C.; Liu, Q.; Xiao, K.; Qian, G. Driving forces of impervious surface in a world metropolitan area, Shanghai: Threshold and scale effect. *Environ. Monit. Assess.* **2019**, *191*, 771. [CrossRef] [PubMed]
33. Zou, Z.; Zhao, X.; Liu, S.; Zhou, C. Driving Forces and Future Scenario Simulation of Urban Agglomeration Expansion in China: A Case Study of the Pearl River Delta Urban Agglomeration. *Remote Sens.* **2025**, *17*, 2455. [CrossRef]
34. Yao, L.; Luo, R. Decoding China's urban agglomerations policies: A scientific evaluation and exploration of economic benefits. *Habitat Int.* **2024**, *152*, 103159. [CrossRef]
35. Zhang, X.; Wang, X.; Liu, J. Spatial–Temporal Evolution and Influential Factors of Eco-Efficiency in Chinese Urban Agglomerations. *Sustainability* **2023**, *15*, 12225. [CrossRef]
36. Wang, C.; Liu, H.; Zhang, M. Exploring the mechanism of border effect on urban land expansion: A case study of Beijing-Tianjin-Hebei region in China. *Land Use Policy* **2020**, *92*, 104424.
37. Yin, C.; Chen, R.; Xiao, X.; Qin, Y.; Meng, F.; Yao, Y.; Pan, L.; Zheng, L. Spatio-temporal evolution of vertical urban growth in China's Yangtze River Delta from 1990 to 2020. *Land Use Policy* **2025**, *153*, 107542. [CrossRef]
38. Yin, Z.; Zhou, T.; Li, H.; Xie, S.; Ren, Y. Study on Impervious Surface Change and Urban Expansion of the Guangdong-Hongkong-Macao Greater Bay Area. *Geogr. Geo-Inf. Sci.* **2021**, *37*, 106–113.
39. Li, H.; Yang, D.; Zhu, Z.; Wei, Y.; Zhou, Y.; Ishidaira, H.; Commey, N.A.; Cheng, H. Flood Risk Analysis of Urban Agglomerations in the Yangtze River Basin Under Extreme Precipitation Based on Remote Sensing Technology. *Remote Sens.* **2024**, *16*, 4289. [CrossRef]
40. Chen, D.; Yang, X.; Li, X.; Fu, H.; Duan, Y. Quantifying urban land expansion using remote sensing data and multi-evaluation indices in the Lower Yellow River, China. *Environ. Sustain. Indic.* **2025**, *26*, 100643. [CrossRef]
41. Zhao, S.; Zhou, D.; Zhu, C.; Qu, W.; Zhao, J.; Sun, Y.; Huang, D.; Wu, W.; Liu, S. Rates and patterns of urban expansion in China's 32 major cities over the past three decades. *Landsc. Ecol.* **2015**, *30*, 1541–1559. [CrossRef]
42. Su, S.; Xiao, R.; Jiang, Z.; Zhang, Y. Characterizing landscape pattern and ecosystem service value changes for urbanization impacts at an eco-regional scale. *Appl. Geogr.* **2012**, *34*, 295–305. [CrossRef]
43. Zheng, Y.; Cai, Y.; Yang, K.; Fan, M.; Fu, M.; Wei, C. Quantitative spatiotemporal evolution of large urban agglomeration expansion based on 1995–2020 nighttime light and spectral data. *Ecol. Inform.* **2024**, *84*, 102824. [CrossRef]
44. Hanberry, B.B. Imposing consistent global definitions of urban populations with gridded population density models: Irreconcilable differences at the national scale. *Landsc. Urban Plan.* **2022**, *226*, 104493. [CrossRef]
45. Shao, D.; Zoh, K.; Liu, H. Spatial Expansion and Driving Mechanisms of the Yangtze River Delta, Based on RF-RFECV Feature Selection and Night-Time Light Remote Sensing Data. *Remote Sens.* **2026**, *18*, 1033. [CrossRef]
46. Xia, Y.; Guan, Y.; Yang, T.; Qian, J.; Wei, Z.; Yao, W.; Deng, R.; Zhang, C.; Guo, S. Spatiotemporal Trends and Driving Factors of Global Impervious Surface Area Changes from 2001 to 2020. *Remote Sens.* **2025**, *17*, 3309. [CrossRef]
47. Li, S.; Guo, H.; Sun, Z.; Liu, Z.; Jiang, H.; Zhang, H. Patterns of Typical Chinese Urban Agglomerations Based on Complex Spatial Network Analysis. *Remote Sens.* **2023**, *15*, 920. [CrossRef]
48. Xie, S.; Luo, L.; Wang, H.; Ouyang, M. Spatiotemporal expansion patterns of urban centers since 1975 in China. *Cities* **2026**, *174*, 107009. [CrossRef]
49. Yan, S.; Hu, M.; Ma, X.; Li, X. Exploring the nexus between spatial configuration of urban agglomerations and land use efficiency: A bidimensional analysis considering transport network connectivity. *Cities* **2025**, *167*, 106353. [CrossRef]
50. Huang, D.; Xiao, G. Morphological landscape expansion index: Integrating mathematical morphology and landscape connectivity to decipher urban expansion dynamics. *Ecol. Indic.* **2025**, *179*, 114257. [CrossRef]
51. Sharma, G.K.; Ghuge, V.V. Assessment of urban growth dynamics using landscape expansion index: A study of 514 metropolitan cities from 1975 to 2020. *Land Use Policy* **2025**, *153*, 107557. [CrossRef]
52. Li, X.; Zhang, L.; Liang, C. A GIS-based buffer gradient analysis on spatiotemporal dynamics of urban expansion in Shanghai and its major satellite cities. *Procedia Environ. Sci.* **2010**, *2*, 1139–1156. [CrossRef]
53. Liu, X.; Li, X.; Chen, Y.; Tan, Z.; Li, S.; Ai, B. A new landscape index for quantifying urban expansion using multi-temporal remotely sensed data. *Landsc. Ecol.* **2010**, *25*, 671–682. [CrossRef]
54. Jiao, L.; Mao, L.; Liu, Y. Multi-order Landscape Expansion Index: Characterizing urban expansion dynamics. *Landsc. Urban Plan.* **2015**, *137*, 30–39. [CrossRef]

55. Liu, J.; Jiao, L.; Zhang, B.; Xu, G.; Yang, L.; Dong, T.; Xu, Z.; Zhong, J.; Zhou, Z. New indices to capture the evolution characteristics of urban expansion structure and form. *Ecol. Indic.* **2021**, *122*, 107302. [CrossRef]
56. Yang, J.; Huang, X. The 30 m annual land cover dataset and its dynamics in China from 1985 to 2024. *Earth Syst. Sci. Data* **2025**, *13*, 3907–3925. [CrossRef]
57. Chen, M.; Chen, L.; Xian, Y.; Cheng, J.; Liang, L.; Ma, J. Evolution of urbanized area's entities and fow space towards high-quality development path in China. *Bull. Chin. Acad. Sci.* **2023**, *38*, 1950–1961.
58. Chen, D.; Zhang, F.; Jim, C.Y.; Bahtebay, J. Spatio-temporal evolution of landscape patterns in an oasis city. *Environ. Sci. Pollut. Res.* **2023**, *30*, 3872–3886.
59. Zhang, M.; Ning, L.; Li, J.; Wang, Y. Study on Spatial Pattern Changes and Driving Factors of Land Use/Cover in Coastal Areas of Eastern China from 2000 to 2022: A Case Study of Jiangsu Province. *Land* **2025**, *14*, 2031. [CrossRef]
60. Xiong, S.; Zhang, X.; Wang, H.; Meng, Q.; Du, S. 40-year (1984–2024) mapping of urban land use dynamics in China. *Sci. Bull.* **2026**, *71*, 1474–1485. [CrossRef] [PubMed]
61. Dong, H.; Li, R.; Li, J.; Li, S. Study on Urban Spatiotemporal Expansion Pattern of Three First-class Urban Agglomerations in China Derived from Integrated DMSP-OLS and NPP-VIIRS Nighttime Light Data. *J. Geo-Inf. Sci.* **2020**, *22*, 1161–1174. [CrossRef]
62. Jiao, L.; Liu, J.; Xu, G.; Dong, T.; Gu, Y.; Zhang, B.; Liu, Y.; Liu, X. Proximity Expansion Index: An improved approach to characterize evolution process of urban expansion. *Comput. Environ. Urban Syst.* **2018**, *70*, 102–112. [CrossRef]

Disclaimer/Publisher's Note: The statements, opinions and data contained in all publications are solely those of the individual author(s) and contributor(s) and not of MDPI and/or the editor(s). MDPI and/or the editor(s) disclaim responsibility for any injury to people or property resulting from any ideas, methods, instructions or products referred to in the content.